Correction of the Disease Phenotype of Myocilin-Causing Glaucoma by a Natural Osmolyte

Li-Yun Jia,[1,2,3] *Bo Gong,*[1] *Chi-Pui Pang,*[1] *Yao Huang,*[2] *Dennis Shun-Chiu Lam,*[1] *Ningli Wang,*[*,2] *and Gary Hin-Fai Yam*[*,1]

Purpose. To characterize a novel Asp384Asn (D384N) mutant myocilin (MYOC) that causes juvenile-onset open-angle glaucoma (JOAG) and investigate the correction of mutant phenotype by a natural osmolyte, trimethylamine *N*-oxide (TMAO).

Methods. A Chinese JOAG family was recruited and genomic DNA was extracted from peripheral blood obtained from 44 family members. Coding regions of the *MYOC* were sequenced. Two hundred individuals (>60 years old) without ocular hypertension or glaucoma were the control subjects. Full-length human wild-type *MYOC* cDNA was cloned in p3xFLAG-myc-CMV-25 and missense mutation was introduced by site-directed mutagenesis. Transfected human trabecular meshwork cells were treated with small-molecule chemical chaperones. Secreted MYOC was analyzed by combined immunoprecipitation-Western blot analysis. Intracellular myocilin was fractionated into Triton X-100-soluble and insoluble fractions, and analyzed by Western blot analysis. Intracellular aggregate and apoptosis were assayed by immunofluorescence. The effect of TMAO on subcellular myocilin distribution was analyzed by density gradient fractionation, followed by Western blot analysis.

Results. A novel c.1150G>A change of *MYOC* was identified. Screening of optineurin, *WDR36*, and *CYP1B1* showed an absence of disease-causing polymorphisms. Mutated D384N myocilin had reduced solubility and was aggregation-prone and nonsecreted. Treatment of transfected cells with TMAO improved the solubility of the D384N mutant, which was corrected for secretion in a dose–response manner. TMAO reduced the distribution of the D384N mutant in the endoplasmic reticulum (ER), alleviated ER stress, and rescued cells from apoptosis.

Conclusions. The results indicate that TMAO, with chaperoning activity, facilitated the folding and secretion of mutant MYOC. This therapeutic approach assisted by a chemical chaperone can be developed for treating glaucoma. (*Invest Ophthalmol Vis Sci.* 2009;50:3743–3749) DOI:10.1167/iovs.08-3151

Glaucoma is a heterogeneous group of optic neuropathies characterized by degeneration of retinal ganglion cells and the optic nerve.[1] It is a leading cause of irreversible blindness affecting more than 70 million people worldwide.[2] Primary open-angle glaucoma (POAG) is a common form, accounting for more than half of all cases.[3] Juvenile-onset open-angle glaucoma (JOAG) appears early in life (before 40 years old) and is transmitted in an autosomal-dominant inheritance fashion. To date, 23 genetic loci have been mapped and three genes identified: myocilin (*MYOC*), optineurin (*OPTN*), and WD repeat domain 36 (*WDR36*). *MYOC* mutations are associated with high intraocular pressure (IOP) in POAG and account for up to 35% juvenile-onset and 4% adult-onset POAG.[4] Most glaucoma-causing *MYOC* mutations are located the in olfactomedin-like domain of the encoded protein (Human Gene Mutation Database http://www.hgmd.cf.ac.uk/ac/gene.php?gene MYOC). The MYOC protein is expressed in various ocular tissues and abundantly in trabecular meshwork (TM) cells. With the coiled–coil domain, it interacts with different extracellular matrix components.[5,6] MYOC expression has been shown to differentially regulate cell adhesion genes and cell–matrix interactions, suggesting a possible functional role in intercellular regions.[7] In TM tissues of patients with POAG, it is present in microfibrillar structure and sheath-derived plaque materials.[8]

Most glaucoma-causing MYOC mutants are misfolded, detergent-insoluble, and aggregation-prone and are retained in the endoplasmic reticulum (ER).[9,10] Despite wild-type (WT) MYOC, which does not have a proven function, the mutants may cause glaucoma by a pathologic gain of function. We and other groups have reported that several missense and truncated MYOC mutants form hetero-oligomeric complexes with WT MYOC and aggregate intracellularly, resulting in secretion blockade.[10–13] Formation of inclusion bodies typical of Russell bodies confirm ER overloading, which induce an unfolded protein response (UPR) and result in apoptosis.[13] This cell death mechanism could explain the fewer TM cells in patients with MYOC-caused glaucoma.[12] The phagocytic capacity of the remaining TM population would be insufficient for the effective cleaning of aqueous humor, thus leading to elevation of IOP.[14]

The success of chemical chaperones to correct a variety of misfolded proteins associated with pathologic conditions has made the chaperone-assisted therapy an appealing therapeutic approach for protein-folding diseases. We have shown that 4-phenylbutyric acid (4-PBA) corrects ER-retained aggregated MYOC mutants (C245Y, P370L, and Y437H) for intracellular trafficking and this action rescues the affected cells from apoptosis.[15] We report a novel *MYOC* missense mutation in a Chinese family and the in vitro effects of trimethylamine *N*-oxide (TMAO), a small-molecule, natural osmolyte capable of stabilizing protein folding.

From the [1]Department of Ophthalmology and Visual Sciences, The Chinese University of Hong Kong, Hong Kong, China; and the [2]Department of Ophthalmology, Beijing Tongren Hospital, Capital University of Medical Sciences, Beijing, China.

[3]Present affiliation: Peking University People's Hospital, Beijing, China.

Supported by Direct Grant 2041361 from the Medical Panel, The Chinese University of Hong Kong and Beijing Natural Science Foundation, China.

Submitted for publication November 12, 2008; revised January 23, 2009; accepted May 4, 2009.

Disclosure: **L.-Y. Jia**, None; **B. Gong**, None; **C.-P. Pang**, None; **Y. Huang**, None; **D.S.-C. Lam**, None; **N. Wang**, None; **G.H.-F. Yam**, None

The publication costs of this article were defrayed in part by page charge payment. This article must therefore be marked "*advertisement*" in accordance with 18 U.S.C. §1734 solely to indicate this fact.

*Each of the following is a corresponding author: Gary H.-F. Yam, Department of Ophthalmology and Visual Sciences, The Chinese University of Hong Kong, Hong Kong, China; gary_yam@cuhk.edu.hk.
Ningli Wang, Department of Ophthalmology, Beijing Tongren Hospital, Capital University of Medical Sciences, Beijing, China; wningli@vip.163.com.

Materials and Methods

Patient Recruitment

The study protocol was approved by The Ethics Committee for Human Research, Beijing Tongren Hospital, Capital Medical University and adhered to the tenets of the Declaration of Helsinki. A Chinese JOAG family attending the Eye Centre, Beijing Tongren Hospital, participated in the study. Informed consent and complete ophthalmic examination for each patient or family member were obtained. IOP was measured by applanation tonometry and visual field perimetry (Humphrey perimeter with Glaucoma Hemifield Test; Carl Zeiss Meditec, Inc. Dublin, CA). Patients received the diagnosis of JOAG before 40 years of age. They showed IOP higher than 22 mm Hg in both eyes, open anterior chamber angles (grade 3 or 4 by gonioscopy), characteristic optic disc damage, and typical visual field loss without secondary causes (including trauma, uveitis or steroid-induced glaucoma). Patients with IOP higher than 22 mm Hg but no visual field impairment received a diagnosis of ocular hypertension (OHT). Two hundred individuals (older than 60 years) without OHT or POAG were normal control subjects.

Mutation Analysis

Peripheral blood from 44 family members was collected for genomic DNA extraction. Complete coding regions of *MYOC* were sequenced. Also genotyped were three single nucleotide polymorphisms (SNPs) in *OPTN* (M98K, IVS5+38T>G, IVS8-53T>C) and one SNP in *WDR36* (IVS5+30C>T). Data were compared with sequences from GenBank (AB006686S, AF420371, and NM139281; http://www.ncbi.nlm.nih.gov/Genbank; provided in the public domain by the National Center for Biotechnology Information, Bethesda, MD).

Expression Constructs, Mutagenesis, and Transfection

Full-length WT *MYOC* cDNA from human skeletal muscle was cloned to p3xFLAG-myc-CMV-25 (Sigma-Aldrich, St. Louis, MO) to generate pFLAG-myc-MYOC^{WT}.[15] Single base change was introduced by site-directed mutagenesis (QuikChange II; Stratagene, La Jolla, CA) with specific oligonucleotides (sense, 5′-CGG ACA TTG ACT TGG CTG TGA ATG AAG CAG GCC TCT GGG TC, altered base is underscored) and verified by sequencing. Human trabecular meshwork (HTM) cells[15] were transfected with 1 μg plasmid DNA (FuGene HD reagent; Roche Diagnostics, Basel, Switzerland).

Low Temperature or Chemical Chaperone Treatments

Transfected cells were incubated at 37°C or 30°C, 1 mM 4-PBA (triButyrate, Triple Crown America, Inc., Perkasie, PA) or 25 to 200 mM TMAO (Sigma-Aldrich) for 48 hours.

MYOC Secretion and Solubility

Culture medium was immunoprecipitated with rabbit polyclonal antibody against myc (Santa Cruz Biotech, Santa Cruz, CA) bound to protein A beads (Dynabead; Dynal-Invitrogen, Carlsbad, CA) and analyzed by Western blot analysis for FLAG. After they were washed, the cells were lysed in Triton X-100 (Tx) lysis buffer at 5×10^6 cells/mL for 2 minutes on ice.[15,16] After centrifugation, Tx-soluble and insoluble fractions were analyzed by Western blot analysis using mouse monoclonal anti-GAPDH-horseradish peroxidase (HRP) conjugate (Sigma-Aldrich), anti-β-actin-HRP conjugate (Sigma-Aldrich) and anti-FLAG-HRP conjugate for MYOC (Sigma-Aldrich), followed by enhanced chemiluminescence (Amersham, Bucks, UK). Band intensity was then analyzed with image-analysis software (Quantity One Image Analysis; BioRad, Hercules, CA). MYOC expression was normalized with GAPDH for Tx-soluble protein or β-actin for Tx-insoluble protein.

MYOC Transcription

Total RNA was obtained by a RNA purification kit (RNeasy kit; Qiagen, Valencia, CA) and an on-column DNase digestion kit (RNase-free DNase kit; Qiagen). cDNA from 1 μg RNA, 10 ng/mL random hexanucleotide primer (Invitrogen) and reverse transcriptase (SuperScript III; Invitrogen) was amplified for *MYOC* and *GAPDH*.[15]

Unfolded Protein Response

Cells were lysed in RIPA buffer and soluble protein was analyzed by Western blot analysis with mouse monoclonal anti-BiP antibody (BD Bioscience, San Jose, CA), GAPDH-HRP and β-actin-HRP, respectively, followed by ECL.

Apoptosis Assay

Cells were fixed and stained with a monoclonal antibody against FLAG (Sigma-Aldrich) and red X-conjugated secondary antibody (Jackson ImmunoResearch Laboratory, West Grove, PA).[17] Nuclei were stained with DAPI. Samples were examined by fluorescence microscopy (DMRB; Leica, Wetzlar, Germany) equipped with a color imaging system (Spot RT; Diagnostic Instruments, Sterling Heights, MI). The apoptosis rate was represented as the percentage of cells with fragmented nuclei. For each experiment ($n = 3$), 10 random images (×40 objective) were analyzed.

Density Gradient and Protein Analysis

Stable transfectant were selected by 800 μg/mL geneticin (Geneticin 418; Invitrogen) for 10 days. Cells treated with chemical chaperones for 2 days were collected in 250 mM sucrose buffer containing 10 mM HEPES-NaOH (pH 7.4), 1 mM EDTA.Na_2 and protease inhibitor, homogenized and spun at 1500*g* to remove the nuclei (Dounce; Bellco Glass Co., Vineland, NJ). The supernatant was further spun at 65,000*g* for an hour. The clear supernatant contained cytoplasmic soluble protein (see Fig. 5, fraction 1). Pellet containing cytoplasmic organelles was layered on top of a density gradient (Optiprep 2.5%–30%; Nycomed, Oslo, Norway) and spun at 100,000*g* for 2 hours. Fractions 2 to 8 (according to Optiprep density) were analyzed by Western blot analysis with anti-FLAG-HRP, monoclonal anti-calnexin (BD Bioscience), polyclonal anti-GM130 antibody (Santa Cruz Biotechnology), and detected by ECL.

Results

Mutation Analysis

Nine family members had JOAG and two had OHT (Fig. 1A). The proband (IV:6) showed A glaucomatous phenotype at 25 years of age with IOP higher than 23 mm Hg, cup-disc ratio 0.9, open chamber angle grade 3 (Shaffer), and typical glaucomatous visual field loss in both eyes. No anterior segment change was observed. Her mother (III:5) had OHT and normal grade 3 open chamber angle. She maintained her IOP below 17 mm Hg on topical 0.5% timolol maleate twice daily. A missense mutation, c.1150G>A, was identified in the *MYOC* gene in the proband (IV:6) and 12 family members (Figs. 1A, 1B). Eight were confirmed with JOAG (II:1, II:3, III:9, III:14, III:16, III:21, IV:6, and IV:19), two were classified as having suspected glaucoma (III:5 and IV:8), and three young subjects were classified as nonsymptomatic (III:3, IV:5, and IV:11; Table 1). Two hundred unrelated controls did not carry the change. Three reported polymorphisms, −83G>A, 227G>A, and IVS2+35 A>G, were detected but did not segregate with the disease. Screening of *OPTN* and *WDR36* did not show any disease-associated polymorphisms. Three SNPs, 966T>A (M98K), IVS5+38T>G, and IVS8-53T>C, in *OPTN* and IVS5+30C>T in *WDR36* were genotyped but not segregated with JOAG in this family. One family member (III:3, 48 years of age at the time of

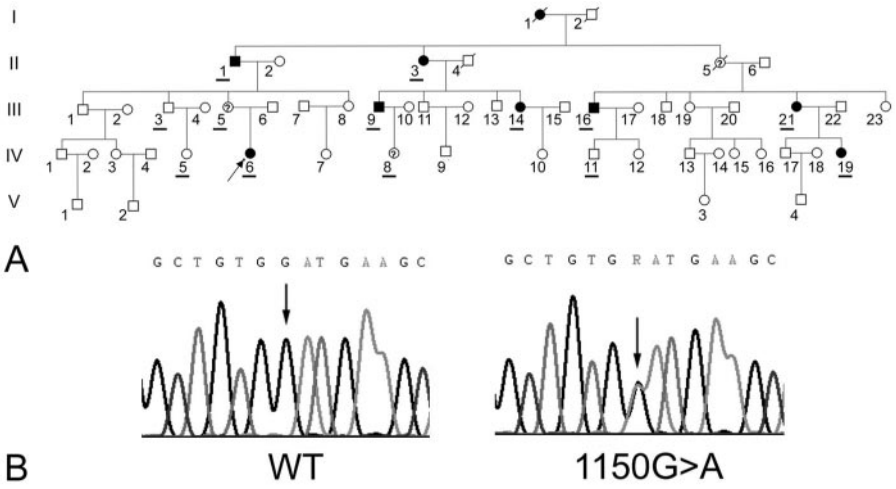

FIGURE 1. (**A**) Pedigree of a Chinese family with JOAG. Persons who were given ophthalmic examination are *underscored* (details in Table 1). *Arrow*: proband (IV:6). All subjects with the c.1150G>A MYOC genotype were heterozygous. (**B**) Sequence alteration of MYOC. Forward sequences showed WT and c.1150G>A. *Arrows*: single base substitution.

inclusion) carrying the c.1150G>A change was asymptomatic with normal IOP levels. This genotype–phenotype variation could be due to the effect of modifier genes, such as *CYP1B1*,[18,19] which is under investigated.

D384N MYOC Solubility and Secretion

The c.1150G>A change led to aspartic acid replaced by asparagine in the 384th amino acid position of the MYOC protein (D384N; GenBank no. AY599652). To test whether the D384N mutant had solubility changes, we transiently transfected pFLAG-myc-MYOC^{WT} or pFLAG-myc-MYOC^{D384N} to HTM cells. Reported MYOC mutants (C245Y, P370L, and Y437H) were used as the control.[15] All recombinant FLAG/myc-MYOC fusion proteins were highly expressed in HTM cells (Fig. 2A). At steady state, approximately 85% of D384N MYOC was resistant to 0.5% Tx extraction compared with approximately 25% of WT. Similarly reduced Tx solubility was found for the C245Y, P370L, and Y437H mutants. Immunofluorescence study showed that D384N MYOC formed cellular aggregates (Fig. 2C), whereas WT had a diffuse vesicular distribution (Fig. 2B). More D384N cells (78% ± 14%) had intracellular MYOC aggregates than did the WT cells (1.4% ± 0.1%; $P < 0.05$, paired Student's *t*-test; Fig. 2D) More D384N cells contained fragmented nuclei (31% ± 3% for D384N and 9% ± 1.5% for the WT; $P < 0.05$, paired Student's *t*-test; Fig. 2D). Unlike the WT, D384N MYOC was secretion defective (Fig. 3A).

Chemical Chaperones Treatment on D384N MYOC Solubility and Secretion

When cells were incubated at 30°C for 2 days, the expression of Tx-soluble D384N MYOC increased (Fig. 3A). The same increase was detected when the cells were treated with 1 mM 4-PBA or 50 mM TMAO. A faint doublet of soluble MYOC seen at 37°C became strongly expressed. Among the treatments, TMAO gave the highest level of Tx-soluble D384N MYOC (~6.2-fold that of the untreated mutant) and approached a level closed to that of the WT. Incubation at 30°C or with 1 mM 4-PBA caused approximately a threefold increase of Tx solubility. Results were reproducible in three different experiments. Combined immunoprecipitation-Western blot analysis showed that incubation at 30°C caused a very minor secretion of D384N MYOC (Fig. 3A). In contrast, more MYOC secretion was found after treatment with the chemical chaperone. Our study did not determine whether 4-PBA or TMAO causes a better extracellular level of mutant MYOC. Instead, we performed IP of media from cultures with the same number of cells and with excessive anti-myc antibody bound to protein A magnetic beads followed by immunoblot analysis with excessive anti-FLAG-HRP antibody. The presence of extracellular MYOC was confirmed by WT MYOC-expressing cells.

TABLE 1. Clinical Information of Family Members with Heterozygous c.1150G>A Change

Subject	Sex/Age at Inclusion	Age of Onset	Highest IOP, Right/Left (mmHg)	Cup-Disc Ratio, Right/Left	Diagnosis	Treatments
II:1	M/89	<35*	38/40	0.9/1.0	JOAG	Trabeculectomy
II:3	F/82	<30*	40/45	1.0/1.0	JOAG	Trabeculectomy
III:3	M/48	NA	18/17	0.2/0.3	Asymptomatic	None
III:5	F/53	36*	24/26	0.3/0.4	OHT	β-Blocker
III:9	M/59	32	50/67	0.9/1.0	JOAG	Trabeculectomy
III:14	F/57	37	47/37	0.8/1.0	JOAG	Trabeculectomy
III:16	M/70	<35*	47/50	1.0/1.0	JOAG	Trabeculectomy
III:21	F/70	<38*	29/35	1.0/0.9	JOAG	Trabeculectomy
IV:5	F/19	NA	15/14	0.3/0.3	Asymptomatic	None
IV:6	F/31	21	23/22	0.9/1.0	JOAG	Trabeculectomy/β-blocker
IV:8	F/35	34	32/30	0.8/0.7	JOAG	Latanoprost
IV:11	M/39	NA	14/15	0.3/0.4	Asymptomatic	None
IV:19	F/39	22	33/35	0.9/0.9	JOAG	Trabeculectomy

* The age of onset was estimated according to individual medical history.

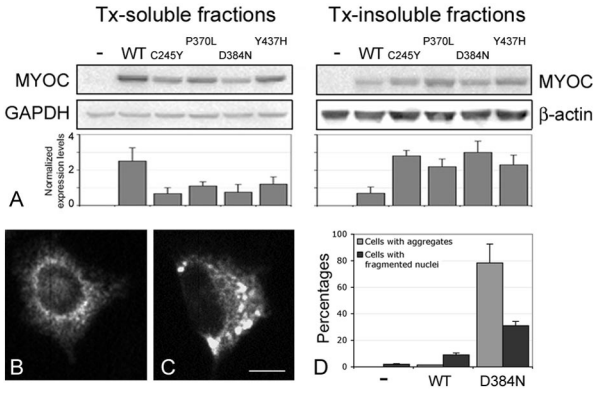

FIGURE 2. Characterization of FLAG/myc-D384N mutant MYOC. (**A**) Western blot analysis of FLAG showed reduced Tx solubility of D384N MYOC. The solubility change was similar to C245Y, P370L, and Y437H MYOC. GAPDH and β-actin were the housekeeping genes in the Tx-soluble and -insoluble fractions, respectively. Quantification by band densitometry indicated the predominant expression of Tx-insoluble mutant MYOC. WT, cells transfected with WT MYOC; −, cells transfected with vector only. (**B**, **C**) Immunofluorescence of WT (**B**) and D384N MYOC (**C**) in HTM cells. Scale bar: 10 μm. (**D**) A histogram showing percentage of transfected cells with MYOC aggregates and fragmented nuclei. −, cells transfected with vector only.

Chemical Chaperones Treatment on Apoptosis

An examination of the percentage of FLAG-positive cells with fragmented nuclei showed that D384N MYOC cells had an apoptosis rate of 31% ± 3.3% (WT cells had a rate of 9% ± 1.5%; Fig. 3D). After the cells were incubated with 50 mM TMAO for 2 days, the rate was reduced to 15.5% ± 2.5% (Fig. 3D). Treatment with 1 mM PBA mildly reduced the apoptosis rate to 20.5% ± 1.5% and low-temperature (30°C) treatment maintained the apoptosis rate at 28.7% ± 2.3%. The rate for untreated mock-transfected HTM cells was 2% ± 0.5%.

Dose-Responsive Effect of TMAO on D384N MYOC Solubility and Secretion

When applied at concentrations higher than 25 mM, TMAO enhanced D384N MYOC solubility, with the highest level at the 100-mM concentration (Fig. 4A). The secretion was also improved. From 5×10^6 cells, incubation with TMAO at 25 mM or higher caused mutant MYOC secretion; peak secretion level was attained with 50 to 100 mM TMAO (Fig. 4B). TMAO at 200 mM did not induce more secretion. Semiquantitative RT-PCR analysis did not reveal any changes in the steady state *MYOC* expression when cells were treated with up to 200 mM TMAO (Fig. 4C). In our further experiments, a lower dose of TMAO (50 mM) with sufficient corrective ability to the secretion defect of D384N MYOC was used.

TMAO on Unfolded Protein Response

HTM cells expressing D384N MYOC for 2 days showed BiP upregulation ~2.5-fold that in WT MYOC cells (Fig. 4D). Treatment with 50 mM TMAO caused further BiP upregulation, greater than that recorded after incubation at 30°C or with 4-PBA.

TMAO on Subcellular Distribution of D384N MYOC

HTM cells stably expressing FLAG/myc-MYOC (WT or D384N) were treated with 50 mM TMAO for 2 days, followed by separation of cytoplasmic fractions by density gradient (0%–30% Optiprep; Nycomed). Collected fractions were immunoblotted for FLAG (representing MYOC), ER lectin calnexin, and Golgi protein GM130. The D384N mutant was restricted to fractions immunoreactive to calnexin and was not in fractions with GM130 (Fig. 5), whereas WT MYOC was distributed in a broader pattern along the gradient that was positive for calnexin and GM130. Moreover, the D384N mutant was not detectable in the cytoplasmic soluble protein (fraction 1), which showed intense immunoreactivity for WT MYOC. Treat-

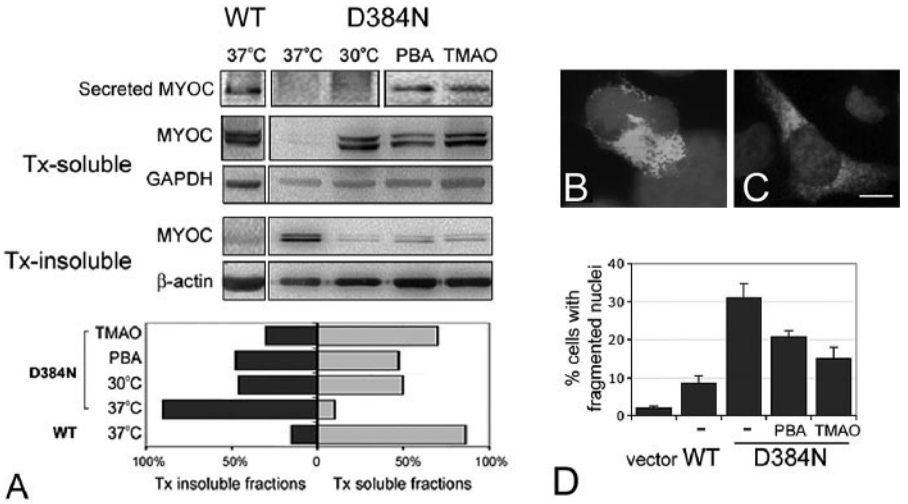

FIGURE 3. Improvement of secretion and Tx solubility of D384N MYOC. (**A**) D384N-transfected cells were incubated at 30°C or treated with chemical chaperones (1 mM 4-PBA and 50 mM TMAO) for 2 days. By combined immunoprecipitation-Western blot analysis, D384N MYOC was detectable in the culture medium after TMAO and 4-PBA treatments. Incubation at 30°C did not show MYOC secretion. Increased expression of the Tx-soluble mutant MYOC was found after treatments. Results were compared to untreated cells expressing mutant or WT MYOC. (**B**, **C**) Immunofluorescence of FLAG (representing MYOC) and DAPI in untreated D384N cells (**B**) and TMAO-treated D384N cells (**C**). Scale bar: 5 μm. (**D**) Apoptosis rates determined by the percentage of cells with fragmented nuclei. TMAO treatment for 2 days resulted in more of a reduction of apoptosis than did 4-PBA.

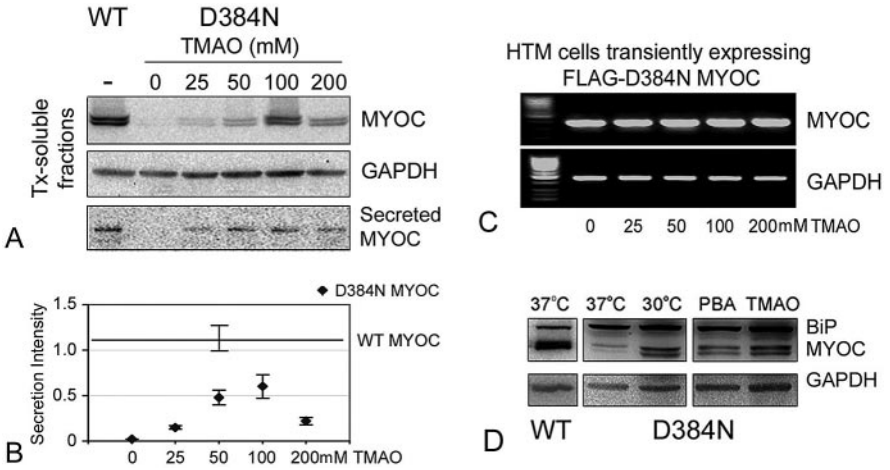

FIGURE 4. TMAO improved Tx solubility and secretion of D384N MYOC. (**A**) HTM cells (2×10^6 cells) transiently expressing FLAG/myc-WT or D384N MYOC were treated with different doses of TMAO (0–200 mM) for 2 days. Tx-soluble fractions were assayed for FLAG (MYOC) and GAPDH. Untreated WT-expressing cells were used as the control. Culture media were collected and IP for myc, followed by Western blot analysis for FLAG for MYOC secretion. (**B**) Band densitometry showed that 50 to 100 mM TMAO improved the secretion of D384N MYOC to a level about half of WT MYOC. (**C**) RT-PCR analysis showed no transcriptional changes of MYOC by TMAO treatment (0–200 mM). GAPDH expression served as the internal control for sample loading. (**D**) TMAO (50 mM) caused BiP upregulation in D384N MYOC cells.

ment with 50 mM TMAO for 2 days resulted in a redistribution of the D384N mutant resembling that of WT. Mutant protein was co-distributed in GM130-positive fractions and reappeared in the cytoplasmic soluble fraction.

DISCUSSION

Many mutations do not cause disease through impaired synthesis of a polypeptide, but produce a protein that cannot fold properly[20–22] and thus lead to disruption of normal functions. Inside cells, there exists stringent protein quality control in the ER-Golgi region to monitor the folding of secretory and membrane proteins.[23,24] In addition to molecular chaperones and enzymes aiding the folding of peptides,[25,26] various machinery proteins are involved in the recognition and retention of aberrant proteins.[27–29] With the impairment of recognition and retrotranslocation for the ubiquitin-proteasome degradation pathway, altered biophysical properties or interactions with other proteins, misfolded proteins are mistrafficked and accumulate in the ER. The consequences are ER stress and UPR. Loss of function of mutant protein and/or its aggregate formation (pathologic gain-of-function) leads to the development of diseases.[30–32]

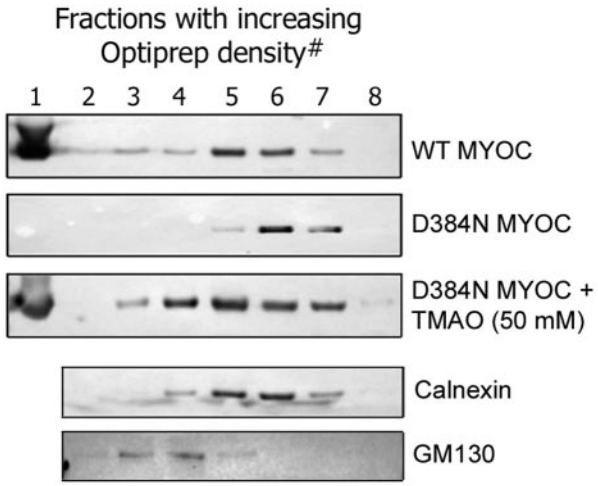

FIGURE 5. TMAO altered the subcellular distribution of D384N MYOC. Unlike WT MYOC with broad distribution and presence in the cytosolic fraction (*lane 1*), untreated D384N mutant mainly co-migrated with calnexin (*lanes 4–7*). No immunoreactivity was detected in GM130-positive fractions (*lanes 2–4*). TMAO-treated mutant MYOC was redistributed in both ER and Golgi-enriched fractions and cytosolic fraction, similar to WT MYOC.

Glaucoma-causing MYOC mutants are mostly misfolded and ER-retained and hence are nonsecreted.[9,10,12,15] Hetero-oligomers formed between mutant and WT MYOC accumulate intracellularly in the form of Russell bodies,[11,13] which further block trafficking of WT MYOC.[10,12] Such ER retention induces UPR, as shown by the upregulation of 78 kDa glucose-regulated protein (BiP) and protein disulfide isomerase, resulting in apoptosis.[9,10,13] In this study, we confirmed the intracellular aggregation and nonsecretion of D384N MYOC, which accounted for IOP-associated JOAG. The mutant protein was Tx-insoluble and only slightly degradable via the ubiquitin-proteasome pathway (data not shown). Upregulation of BiP indicated UPR activation, and the affected cells underwent apoptosis shown by nuclear fragmentations. However, unchanged UPR was observed in transgenic mouse TM tissue expressing mouse MYOC^{Y423H}, which was also intracellularly retained.[33] This could be due to differences between mouse and human MYOC peptide sequences, which share approximately 94% homology. Also, cell stress due to overloading of misfolded protein should be less severe in the mouse and hence, the TM tissue was less susceptible to UPR.

Incubation of cells at 30°C or with chemical chaperones, 4-PBA (1 mM) or TMAO (50 mM), improved Tx solubility of D384N MYOC. However, only chemical chaperone treatment restored its secretion. D384N MYOC remained mostly nonsecreted after low-temperature treatment, which may contribute to the severity of IOP elevation and early disease onset. Vollrath and Liu[34] reported that the degree of mutant secretion at 30°C is inversely related to the severity of the associated glaucoma phenotype. In contrast, chemical chaperones should

be good facilitators of folding of temperature-sensitive mutants. Among the chaperone molecules, TMAO engendered a redistribution of mutant MYOC from the ER. D384N protein was restricted to the density gradient fractions immunoreactive for calnexin, an ER resident protein, whereas WT MYOC was detected in a broader distribution and was not limited to calnexin-positive fractions. On TMAO treatment, D384N mutant was relocalized from the ER-enriched to Golgi-enriched fractions (GM130 positive) and was highly indicative of a reduced ER retention. TMAO also induced further BiP upregulation, indicating UPR induction leading to favorable protein folding in the ER. BiP induction is a major protective mechanism for cells to survive from the ER stress and has implications in organ preservation.[35] As such, the shortened ER retention and activation of UPR could rescue the affected cells from apoptosis. In our different experiments, we found that TMAO treatment corrected the nonsecretion of both mutant and WT MYOC molecules coexpressed in human TM cells (data not shown). Besides, we demonstrated that different severe or mild glaucoma-causing MYOC variants (R82C, C245Y, P370L, T377M, D380A, R422C, R422H, Y437H, I477N, I477S, and N480K) had improved secretion by TMAO treatment and cells were rescued from apoptosis (data not shown).

Setting up a favorable environment for the refolding of improperly folded proteins to their native state has been proposed as a new therapeutic avenue for treating protein-folding diseases.[36,37] Although low temperature can improve protein folding and alleviate abnormal morphology and cell killing induced by misfolded protein expression,[12,34,38] application of low temperature to tissue cells is practically very difficult. Delivery of drugs to target tissue sites is more feasible. Many studies have described the use of cell-permeable small molecules with chaperoning activity to reverse the mislocalization or reduce the aggregation of proteins associated with human diseases.[15,39–49] They include 4-PBA, polyols such as glycerol, trimethylamines such as TMAO, enzyme antagonists, and chemical ligands. The mechanisms of action may involve the stabilization of proteins, prevention of undesirable interactions between proteins, reduction of aggregate formation, and alteration of folding environment or endogenous chaperone activity.[37,50] This gives more efficient transport of client proteins to the intracellular or extracellular destinations. Beside the loss of activity, abnormal protein folding and aggregation can contribute to gain-of-function cytotoxicity.[13,21,47] Hence, correction of protein misfolding or mistrafficking is of critical importance to rescue the damaged cells and relieve the disease severity. Recent reports have substantiated the efficacy of chemical chaperones in alleviating ER stress and apoptosis in lysosomal storage diseases.[17,51,52]

TMAO is a natural osmolyte richly present in deepwater fish, in which high hydrostatic pressure deters protein folding and hence inhibits protein functions. TMAO acts as a protein stabilizer to protect ligand binding and polymerization against pressure inhibition.[53] It improves folding and assembly of different proteins.[41,54,55] It is hydrophobic and is capable of forcing water molecules out of solution onto the protein surface. The increased hydration affects the Gibbs free energy (G) changes along the folding process so that ΔG between native and denatured states becomes larger, thereby driving the equilibrium toward the native state.[56] The solvent-accessible surface area of protein is reduced, and this leads to a tighter packing of protein and stabilization of conformation and enhances the oligomeric assembly.[57] This unique hydrophobic feature makes TMAO more effective than 4-PBA in correcting MYOC folding.[15] Misfolded MYOC may exist in partially denatured or aggregated states. 4-PBA may act by stabilizing the thermolabile mutant MYOC and thus salvage them from denaturation. In the presence of TMAO, driving out water molecules from molten globule structure favors folding into a more native conformation and tighter packing. The mutant amino acid asparagine may lay deep in the protein conformation and is less solvent accessible. Thus, increased hydrostatic pressure caused by TMAO shifts the equilibrium from the improperly folded state to a more native state. This action was evidenced by the correction of aquaporin-2 mutants for functional water channelling activity in mice,[41] formation of histone tetramers,[54] cell surface expression of the functional chloride conductance transporter ΔF508 CFTR,[58] and recovery of trypsin activity.[55] Moreover, the facilitated ER transport of misfolded proteins relieved the ER perturbation and salvaged cells from ER-stress–induced apoptosis.[59,60]

TMAO reduced the ER retention and improved the secretion of D384N mutant MYOC. This alleviated the ER stress and rescued cells from apoptosis. Given that TMAO is a cell-permeable small molecule, it could be applicable for the treatment of MYOC-caused glaucoma through topical administration.

Acknowledgments

The authors thank Thai D. Nguyen for the human trabecular meshwork cell line that was originally established by the late Jon R. Polansky, and the family that participated in the study.

References

1. Morrison JC, Johnson EC, Cepurna W, Jia L. Understanding mechanisms of pressure-induced optic nerve damage. *Prog Retin Eye Res.* 2005;24(2):217–240.
2. Weinreb RN, Khaw PT. Primary open-angle glaucoma. *Lancet.* 2004;363(9422):1711–1720.
3. Klein BEK, Kelin R, Sponsel WE, et al. Prevalence of glaucoma. The Beaver Dam Eye Study. *Ophthalmology.* 1992;99:1499–1504.
4. Fingert JH, Stone EM, Sheffield VC, Alward WL. Myocilin glaucoma. *Surv Ophthalmol.* 2002;47(6):547–561.
5. Joe MK, Sohn S, Choi YR, Park H, Kee C. Identification of flotillin-1 as a protein interacting with myocilin: implications for the pathogenesis of primary open-angle glaucoma. *Biochem Biophys Res Commun.* 2005;336(4):1201–1206.
6. Gobeil S, Letartre L, Raymond V. Functional analysis of the glaucoma-causing TIGR/myocilin protein: integrity of amino-terminal coiled-coil regions and olfactomedin homology domain is essential for extracellular adhesion and secretion. *Exp Eye Res.* 2006;82(6):1017–1029.
7. Paper W, Kroeber M, Heersink S, et al. Elevated amounts of myocilin in the aqueous humor of transgenic mice cause significant changes in ocular gene expression. *Exp Eye Res.* 2008;87(3):245–267.
8. Karali A, Russell P, Stefani F, Tamm E. Localization of myocilin/trabecular meshwork-inducible glucocorticoid response protein in the human eye. *Invest Ophthalmol Vis Sci.* 2000;41:729–740.
9. Jacobson N, Andrews M, Shepard AR, et al. Non-secretion of mutant proteins of the glaucoma gene myocilin in cultured trabecular meshwork cells and in aqueous humor. *Hum Mol Genet.* 2001;10(2):117–125.
10. Joe MK, Sohn S, Hur W, Moon Y, Choi YR, Kee C. Accumulation of mutant myocilins in ER leads to ER stress and potential cytotoxicity in human trabecular meshwork cells. *Biochem Biophys Res Commun.* 2003;312(3):592–600.
11. Gobeil S, Rodrigue MA, Moisan S, et al. Intracellular sequestration of hetero-oligomers formed by wild-type and glaucoma-causing myocilin mutants. *Invest Ophthalmol Vis Sci.* 2004;45(10):3560–3567.
12. Liu Y, Vollrath D. Reversal of mutant myocilin non-secretion and cell killing: implications for glaucoma. *Hum Mol Genet.* 2004;13(11):1193–1204.
13. Yam GHF, Gaplovska-Kysela K, Zuber Ch, Roth J. Aggregated myocilin induces Russell bodies and causes apoptosis: implications for the pathogenesis of myocilin-caused primary open-angle glaucoma. *Am J Pathol.* 2007;170(1):100–109.

14. Matsumoto Y, Johnson DH. Trabecular meshwork phagocytosis in glaucomatous eyes. *Ophthalmologica.* 1997;211(3):147–152.
15. Yam GHF, Gaplovska-Kysela K, Zuber Ch, Roth J. Sodium 4-phenylbutyrate acts as chemical chaperone on misfolded myocilin to rescue cells from endoplasmic reticulum stress and apoptosis. *Invest Ophthalmol Vis Sci.* 2007;48(4):1683–1690.
16. Zhou Z, Vollrath D. A cellular assay distinguishes normal and mutant TIGR/myocilin protein. *Hum Mol Genet.* 1999;8(12):2221–2228.
17. Yam GHF, Zuber Ch, Roth J. A synthetic chaperone corrects the trafficking defect and disease phenotype in a protein misfolding disorder. *FASEB J.* 2005;19:12–18.
18. Bayat, B. Yazdani S, Alavi A, Chiani M, et al. Contributions of MYOC and CYP1B1 mutations to JOAG. *Mol Vis.* 2008;14:508–517.
19. Vasiliou V, Gonzalez FJ. Role of CYP1B1 in glaucoma. *Annu Rev Pharmacol Toxicol.* 2008;48:333–358.
20. Dobson CM. Protein aggregation and its consequences for human disease. *Protein Pept Lett.* 2006;13(3):219–227.
21. Gregersen N. Protein misfolding disorders: pathogenesis and intervention. *J Inherit Metab Dis.* 2006;29(2–3):456–470.
22. Outeiro TF, Tetzlaff J. Mechanisms of disease II: cellular protein quality control. *Semin Pediatr Neurol.* 2007;14(1):15–25.
23. Roth J. Protein N-glycosylation along the secretory pathway: relationship to organelle topography and function, protein quality control and cell interactions. *Chem Rev.* 2002;102:285–303.
24. Moremen KW, Molinari M. N-linked glycan recognition and processing: the molecular basis of endoplasmic reticulum quality control. *Curr Opin Struct Biol.* 2006;16(5):592–599.
25. Fewell SW, Travers KJ, Weissman JS, Brodsky JL. The action of molecular chaperones in the early secretory pathway. *Annu Rev Genet.* 2001;35:149–191.
26. Barral JM, Broadley SA, Schaffar G, Hartl FU. Roles of molecular chaperones in protein misfolding diseases. *Semin Cell Dev Biol.* 2004;15(1):17–29.
27. Helenius A, Aebi M. Roles of N-linked glycans in the endoplasmic reticulum. *Annu Rev Biochem.* 2004;73:1019–1049.
28. McClellan AJ, Tam S, Kaganovich D, Frydman J. Protein quality control: chaperones culling corrupt conformations. *Nat Cell Biol.* 2005;7(8):736–741.
29. Bukau B, Weissman J, Horwich A. Molecular chaperones and protein quality control. *Cell.* 2006;125(3):443–451.
30. Aridor M, Hannan LA. Traffic jams II: an update of diseases of intracellular transport. *Traffic.* 2002;3(11):781–790.
31. Kaufman RJ. Orchestrating the unfolded protein response in health and disease. *J Clin Invest.* 2002;110:1389–1398.
32. Trombetta ES, Parodi AJ. Quality control and protein folding in the secretory pathway. *Annu Rev Cell Dev Biol.* 2003;19:649–676.
33. Gould DB, Reedy M, Wilson LA, Smith RS, Johnson RL, John SW. Mutant myocilin nonsecretion in vivo is not sufficient to cause glaucoma. *Mol Cell Biol.* 2006;26(22):8427–8436.
34. Vollrath D, Liu YH. Temperature sensitive secretion of mutant myocilins. *Exp Eye Res.* 2006;82(6):1030–1036.
35. Lee AS. The ER chaperone and signaling regulator GRP78/BiP as a monitor of endoplasmic reticulum stress. *Methods.* 2005;35(4):373–381.
36. Cohen FE, Kelly JW. Therapeutic approaches to protein-misfolding diseases. *Nature.* 2003;426(6968):905–909.
37. Loo TW, Clarke DM. Chemical and pharmacological chaperones as new therapeutic agents. *Expert Rev Mol Med.* 2007;9(16):1–18.
38. Rennolds J, Boyaka PN, Bellis SL, Cormet-Boyaka E. Low temperature induces the delivery of mature and immature CFTR to the plasma membrane. *Biochem Biophys Res Commun.* 2008;366(4):1025–1029.
39. Brown CR, Hong-Brown LQ, Biwersi J, Verkman AS, Welch WJ. Chemical chaperones correct the mutant phenotype of the delta F508 cystic fibrosis transmembrane conductance regulator protein. *Cell Stress Chaperones.* 1996;1:117–125.
40. Sato S, Ward CL, Krouse ME, Wine JJ, Kopito RR. Glycerol reverses the misfolding phenotype of the most common cystic fibrosis mutation. *J Biol Chem.* 1996;271:635–638.
41. Tamarappoo BK, Verkman AS. Defective aquaporin-2 trafficking in nephrogenic diabetes insipidus and correction by chemical chaperones. *J Clin Invest.* 1998;101(10):2257–2267.
42. Burrows JA, Willis LK, Perlmutter DH. Chemical chaperones mediate increased secretion of mutant alpha 1-antitrypsin (alpha 1-AT) Z: A potential pharmacological strategy for prevention of liver injury and emphysema in alpha 1-AT deficiency. *Proc Natl Acad Sci USA.* 2000;97(4):1796–1801.
43. Bennion BJ, DeMarco ML, Daggett V. Preventing misfolding of the prion protein by trimethylamine N-oxide. *Biochemistry.* 2004;43(41):12955–12963.
44. Bonapace G, Waheed A, Shah GN, Sly WS. Chemical chaperones protect from effects of apoptosis-inducing mutation in carbonic anhydrase IV identified in retinitis pigmentosa 17. *Proc Natl Acad Sci USA.* 2004;101(33):12300–12305.
45. Liu XL, Done SC, Yan K, Kilpelainen P, Pikkarainen T, Tryggvason K. Defective trafficking of nephrin missense mutants rescued by a chemical chaperone. *J Am Soc Nephrol.* 2004;15(7):1731–1738.
46. Ozcan U, Yilmaz E, Ozcan L, et al. Chemical chaperones reduce ER stress and restore glucose homeostasis in a mouse model of type 2 diabetes. *Science.* 2006;313(5790):1137–1140.
47. de Almeida SF, Picarote G, Fleming JV, Carmo-Fonseca M, Azevedo JE, de Sousa M. Chemical chaperones reduce endoplasmic reticulum stress and prevent mutant HFE aggregate formation. *J Biol Chem.* 2007;282(38):27905–27912.
48. Jafarnejad A, Bathaie SZ, Nakhjavani M, Hassan MZ, Banasadegh S. The improvement effect of L-Lys as a chemical chaperone on STZ-induced diabetic rats, protein structure and function. *Diabetes Metab Res Rev.* 2008;24(1):64–73.
49. Mu TW, Jander R. Chemical and biological approaches synergize to ameliorate protein-folding diseases. *Cell.* 2008;134(5):769–781.
50. Papp E, Csermely P. Chemical chaperones: mechanisms of action and potential use. *Handbook Exp Pharmacol.* 2006(172):405–416.
51. Yam GHF, Bosshard N, Zuber Ch, Steinmann B, Roth J. A pharmacological chaperone corrects the lysosomal storage in Fabry disease caused by trafficking-incompetent variants. *Am J Physiol (Cell Physiol).* 2006;290:C1076–C1082.
52. Wei H, Kim SJ, Zhang Z, Tsai PC, Wisniewski KE, Mukherjee AB. ER and oxidative stresses are common mediators of apoptosis in both neurodegenerative and non-neurodegenerative lysosomal storage disorders and are alleviated by chemical chaperones. *Hum Mol Genet.* 2008;17(4):469–477.
53. Yancey PH, Fyfe-Johnson AL, Kelly RH, Walker VP, Aunon MT. Trimethylamine oxide counteracts effects of hydrostatic pressure on proteins of deep-sea teleosts. *J Exp Zool.* 2001;289(3):172–176.
54. Banks DD, Gloss LM. Folding mechanism of the (H3–H4)2 histone tetramer of the core nucleosome. *Protein Sci.* 2004;13(5):1304–1316.
55. Kumar R, Serrette JM, Thompson EB. Osmolyte-induced folding enhances tryptic enzyme activity. *Arch Biochem Biophys.* 2005;436(1):78–82.
56. Qu Y, Bolen CL, Bolen DW. Osmolyte-driven contraction of a random coil protein. *Proc Natl Acad Sci U S A.* 1998;95(16):9268–9273.
57. Shearer AG, Hampton RY. Structural control of endoplasmic reticulum-associated degradation: effect of chemical chaperones on 3-hydroxy-3-methylglutaryl-CoA reductase. *J Biol Chem.* 2004;279(1):188–196.
58. Fischer H, Fukuda N, Barbry P, Illek B, Sartori C, Matthay MA. Partial restoration of defective chloride conductance in DeltaF508 CF mice by trimethylamine oxide. *Am J Physiol Lung Cell Mol Physiol.* 2001;281(1):L52–L57.
59. Shepshelovich J, Goldstein-Magal L, Globerson A, Yen PM, Rotman-Pikielny P, Hirschberg K. Protein synthesis inhibitors and the chemical chaperone TMAO reverse endoplasmic reticulum perturbation induced by overexpression of the iodide transporter pendrin. *J Cell Sci.* 2005;118(8):1577–1586.
60. Mulhern ML, Madson CJ, Kador PF, Randazzo J, Shinohara T. Cellular osmolytes reduce lens epithelial cell death and alleviate cataract formation in galactosemic rats. *Mol Vis.* 2007;13:1397–1405.